Kirchhoff prestack depth migration in velocity models with and without rotation of the tensor of elastic moduli: Poorly displayed part of migrated interface in correct model with triclinic anisotropy

Václav Bucha
Department of Geophysics, Faculty of Mathematics and Physics, Charles University in Prague, Ke Karlovu 3, 121 16 Praha 2, Czech Republic,
E-mail: bucha@seis.karlov.mff.cuni.cz

Summary

We use the Kirchhoff prestack depth migration to calculate migrated images in simple anisotropic homogeneous velocity models in order to show the impact of rotation of the tensor of elastic moduli on migrated images. The recorded wave field is generated in models composed of two homogeneous layers separated by a non-inclined curved interface. The anisotropy of the upper layer is triclinic with and without the rotation of the tensor of elastic moduli. We apply the Kirchhoff prestack depth migration to correct single-layer velocity models with the same triclinic anisotropy (with and without the rotation) as in the upper layer during the calculation of the recorded wave field. We show and discuss unexpected poorly displayed part of the migrated interface in the correct velocity model used for migration.

Keywords

3-D Kirchhoff prestack depth migration, anisotropic velocity model, rotation of the tensor of elastic moduli

1. Introduction

The migrated interface was clear and coincided nearly perfectly with the original interface in all previous migrated images calculated in the correct single-layer velocity models (see Bucha, 2011, 2012a, 2012b, 2013a). In each of these cases, the medium in the velocity model for the migration is equal to the medium in the upper layer of the velocity model used to compute the recorded wave field.

In this paper we show unexpected results of analogous migration in the correct single-layer velocity model with triclinic anisotropy with the rotation of the tensor of elastic moduli around the axis x_2. The angle of rotation is equal to 15 degrees. We observed nearly vanishing part of the migrated interface. To explain the unexpected phenomenon we compare migrated images, seismograms and ray diagrams for selected common-shot. To see distinctly the differences, we compare the results with calculations for the model with different velocity in the bottom layer and for the model without the rotation of the tensor of elastic moduli.

The dimensions of the velocity model, shot-receiver configuration, methods for calculation of the recorded wave field and the Kirchhoff prestack depth migration are the same as in the paper by Bucha (2013a).

In: Seismic Waves in Complex 3-D Structures, Report 23 (Department of Geophysics, Charles University, Prague, 2013), pp. 61–69

2. Anisotropic velocity models

The dimensions of homogeneous velocity models are the same as in the paper by Bucha (2013a). The recorded wave field is computed in the velocity models composed of two layers separated by the same interface as in the paper by Bucha (2013a). We use three velocity models. The first model uses the triclinic anisotropy without the rotation of the tensor of elastic moduli in the upper layer. The second and third models have equal triclinic anisotropy. The tensor of elastic moduli in the upper layer is rotated with respect to the first velocity model by 15 degrees around the x_2 coordinate axis. The second and third models differ by the velocity in the isotropic homogeneous bottom layer.

2.1. Velocity models for the recorded wave field

2.1.1 Anisotropic velocity model without the rotation of the tensor of elastic moduli

Migrated image for this model was calculated earlier in the paper by Bucha (2012a). The medium (TA) in the upper layer is the triclinic medium by Mensch & Rasolofosaon (1997) without the rotation of the tensor of elastic moduli. The matrix of density-reduced elastic moduli A_{ij} in km^2/s^2 reads

$$\begin{pmatrix} 10.3 & 0.9 & 1.3 & 1.4 & 1.1 & 0.8 \\ & 10.6 & 2.1 & 0.2 & -0.2 & -0.6 \\ & & 14.1 & 0.0 & -0.5 & -1.0 \\ & & & 5.1 & 0.0 & 0.2 \\ & & & & 6.0 & 0.0 \\ & & & & & 4.9 \end{pmatrix}. \tag{1}$$

The bottom layer is isotropic and the P-wave velocity is $V_p = 3.6$ km/s.

2.1.2 Two anisotropic velocity models with the rotation of the tensor of elastic moduli

The medium (TA-15) in the upper layer is the triclinic medium by Mensch & Rasolofosaon (1997) rotated by 15 degrees around the coordinate axis x_2 (see Figure 1). The matrix of density-reduced elastic moduli A_{ij} in km^2/s^2 reads

$$\begin{pmatrix} 11.68 & 0.88 & 0.47 & 1.09 & 1.37 & 0.99 \\ & 10.60 & 2.12 & 0.35 & 0.13 & -0.53 \\ & & 14.38 & 0.32 & 0.10 & -0.83 \\ & & & 4.99 & -0.22 & 0.22 \\ & & & & 5.17 & -0.53 \\ & & & & & 5.01 \end{pmatrix}. \tag{2}$$

These two models have different P-wave velocity in the isotropic bottom layer, V_p is either 3.6 or 3.8 km/s.

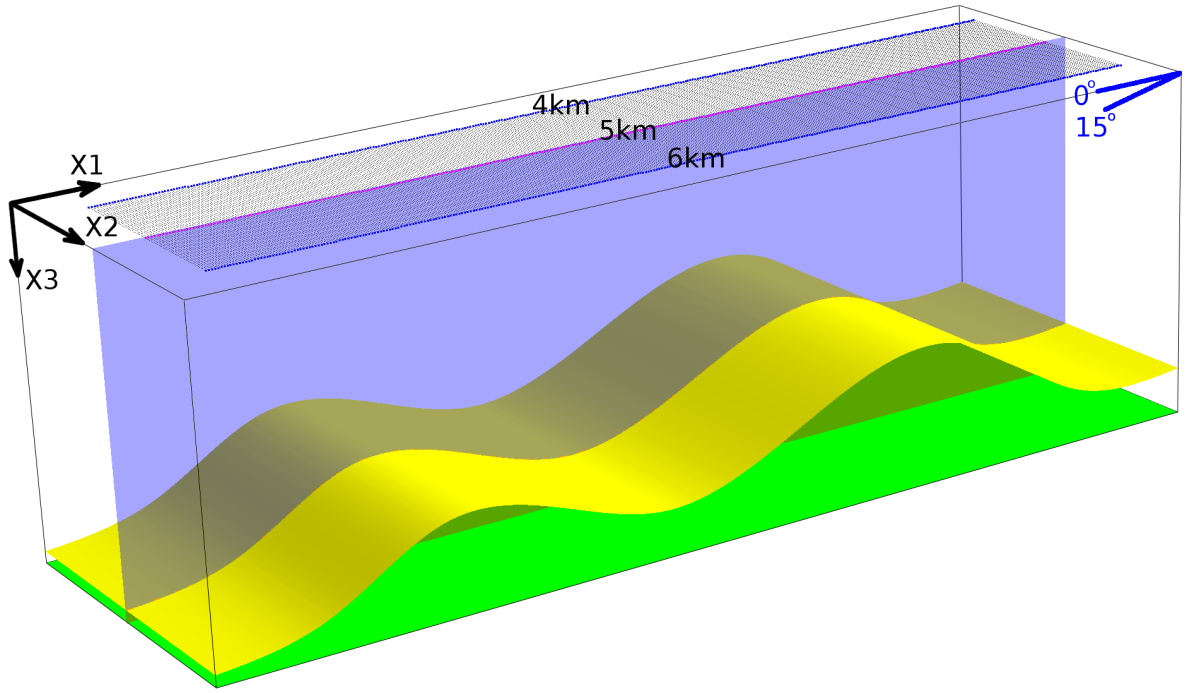

Figure 1. Part of the velocity model with 81 parallel profile lines, the non-inclined curved interface and the bottom velocity model plane. The horizontal dimensions of the depicted part of the velocity model are 9.2 km x 3 km, the depth is 3 km. We compute and stack migrated images in the 2-D plane located in the middle of the shot-receiver configuration, at horizontal coordinate x_2=5 km. The rotation of the tensor of elastic moduli around axis x_2 is equal to 15 degrees.

2.2. Velocity models for the migration

The distribution of elastic moduli in each single-layer velocity model for migration is the same as the distribution in the upper layer of the velocity model used to calculate the corresponding recorded wave field.

3. Migration using the correct velocity models with triclinic anisotropy with and without the rotation of the tensor of elastic moduli

The measurement configuration, calculation of the recorded wave field and the Kirchhoff prestack depth migration are the same as in the paper by Bucha (2013a).

Figure 2a displays the stacked migrated image calculated in the correct velocity model without rotation, specified by matrix (1). In this case the migrated interface is nicely displayed.

Figure 2b shows the stacked migrated image calculated in the correct velocity model without interface, specified by matrix (2), i.e. in the triclinic anisotropy with 15 degree rotation of the tensor of elastic moduli around the x_2 axis. The recorded wave field is calculated in the model with the P-wave velocity in the bottom layer $V_p = 3.6$ km/s. Note the poorly displayed migrated interface in the horizontal range of approximately 4−6 km, and compare with Figure 2a.

To explain the nearly vanishing part of the interface, we calculated and plotted also the common–shot images for shot 80 of profile line $x_2 = 5$ km (Figure 3), corresponding seismograms (Figure 4), and corresponding ray diagrams (Figure 5). We then identified two causes of the poorly displayed part of the migrated interface.

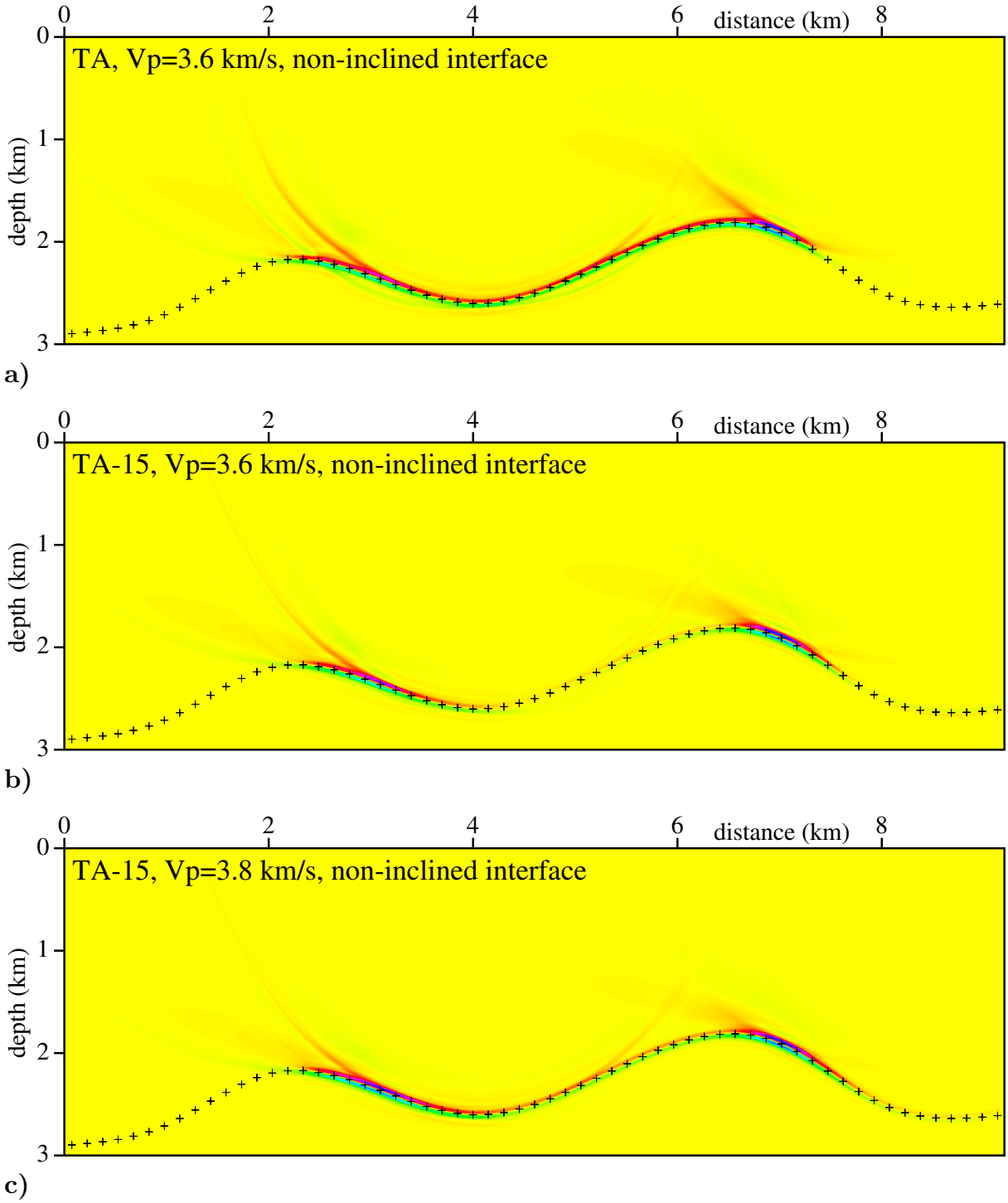

Figure 2. Stacked migrated images calculated in the correct velocity models without interfaces, specified by **a)** triclinic anisotropy without the rotation (seismograms calculated in the model with $V_p = 3.6$ km/s in the bottom layer), **b)** triclinic anisotropy with 15 degree rotation of the tensor of elastic moduli around the x_2 axis (seismograms calculated in the model with $V_p = 3.6$ km/s in the bottom layer), and **c)** triclinic anisotropy with 15 degree rotation of the tensor of elastic moduli around the x_2 axis (seismograms calculated in the model with V_p in the bottom layer increased from 3.6 to 3.8 km/s). The distribution of elastic moduli in the single-layer velocity models for migration is the same as the distribution in the upper layer of the velocity models used to calculate the recorded wave field. 81×240 common-shot prestack depth migrated images, corresponding to 81 profile lines and 240 sources along each profile line, have been stacked. The crosses denote the interface in the velocity models used to compute the recorded wave field.

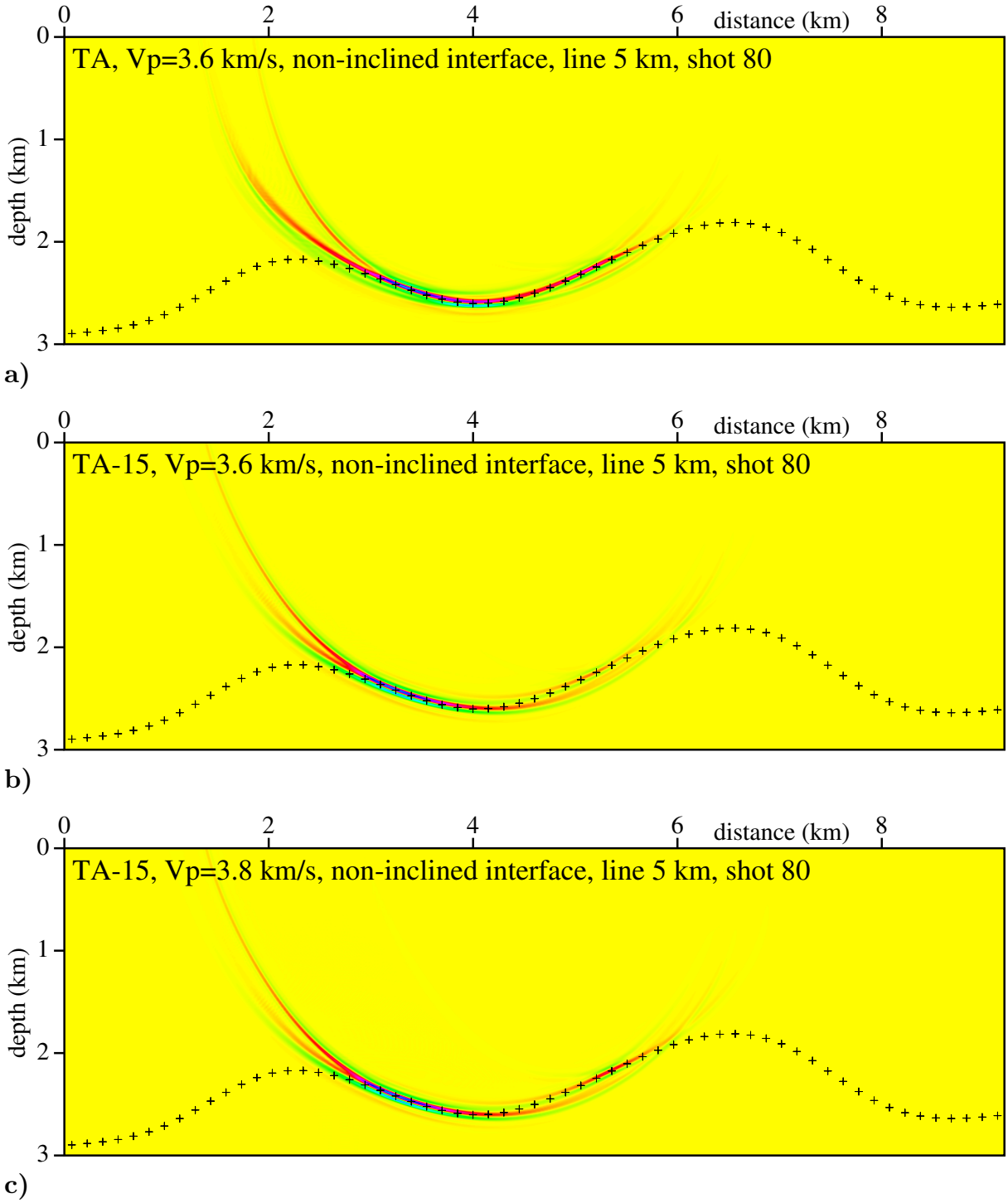

Figure 3. Prestack depth migrated images of the single common-shot gather at line $x_2 = 5$ km corresponding to shot 80 ($x_1 = 4.975$ km), migrated using **a)** triclinic anisotropy without the rotation (seismograms calculated in the model with $V_p = 3.6$ km/s in the bottom layer), **b)** triclinic anisotropy with 15 degree rotation of the tensor of elastic moduli around the x_2 axis (seismograms calculated in the model with $V_p = 3.6$ km/s in the bottom layer), and **c)** triclinic anisotropy with 15 degree rotation of the tensor of elastic moduli around the x_2 axis (seismograms calculated in the model with V_p in the bottom layer increased from 3.6 to 3.8 km/s). The distribution of elastic moduli in the single-layer velocity models for migration is the same as the distribution in the upper layer of the velocity models used to calculate the recorded wave field. The crosses denote the interface in the velocity model used to compute the recorded wave field.

The *first cause* is obvious from the comparison of the seismograms in Figure 4a and Figure 4b. The seismograms for the model with the rotation in Figure 4b clearly display the change of the sign of the reflection coefficient around a region of the nearly vanishing reflection coefficient. The value of P-wave velocity in the bottom layer $V_p = 3.6$ km/s is between the values of horizontal (axis x_1) and vertical (axis x_3) P-wave velocities $V_p^{x_1} = \sqrt{A_{11}}$ and $V_p^{x_3} = \sqrt{A_{33}}$ corresponding to matrix (2). The square roots of elastic moduli are $V_p^{x_1} = 3.42$ km/s and $V_p^{x_3} = 3.79$ km/s. The corresponding common-shot image for shot 80 (Figure 3b) is oriented correctly but the relative amplitude is very small and the image is shorter in comparison with Figure 3a calculated for the model without rotation.

To demonstrate the influence of the nearly vanishing reflection coefficient, we increased the P-wave velocity in the bottom layer from $V_p = 3.6$ km/s to $V_p = 3.8$ km/s. We then performed another calculation in this model with the rotation in the upper layer, specified by matrix (2), and with the increased P-wave velocity in the bottom layer. The increment of velocity changed the reflection coefficient and the amplitudes of seismograms in the discussed region have considerably increased, see Figure 4c. The migrated interface in the horizontal range of approximately $4-6$ km, poorly displayed in the stacked migrated image of Figure 2b, has considerably improved in the new stacked migrated image of Figure 2c. For the comparison of the selected common-shot migrated images refer to Figures 3b and 3c.

The *second cause* of poorly displayed part of the migrated interface is evident from the comparison of the ray diagrams displayed in Figure 5a and Figure 5b. Note the differences in the illumination of the interface by rays. The illuminated part of the interface is smaller in the model with the rotation.

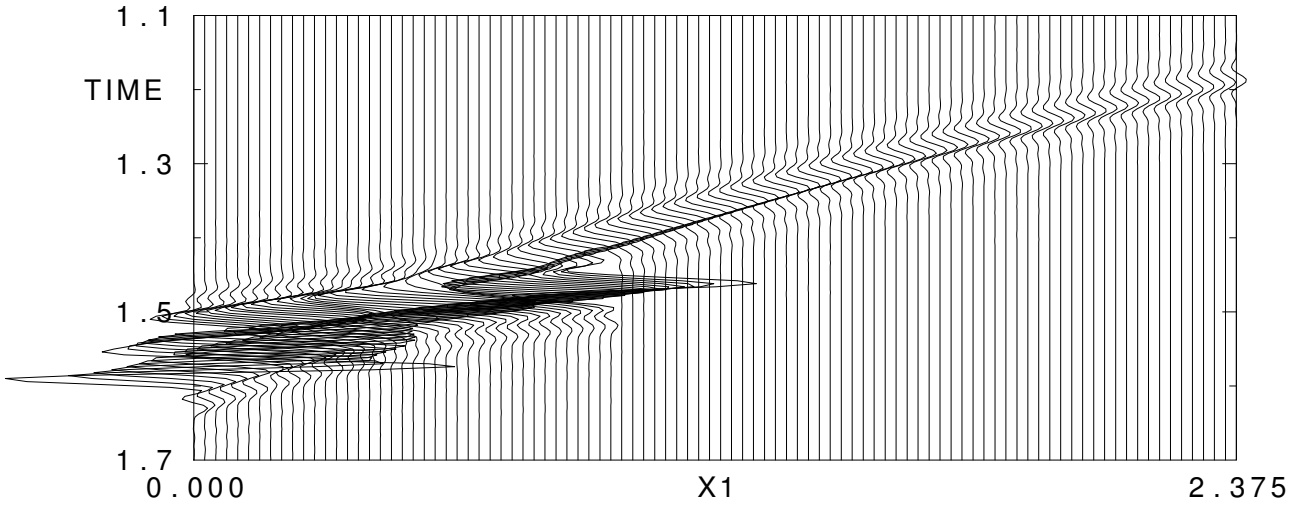

a)

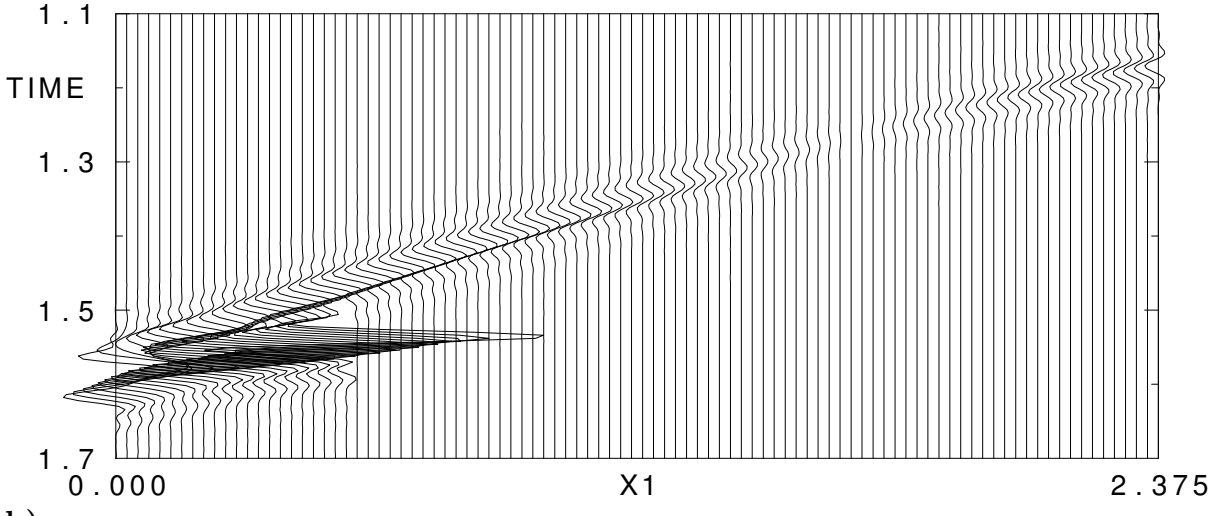

b)

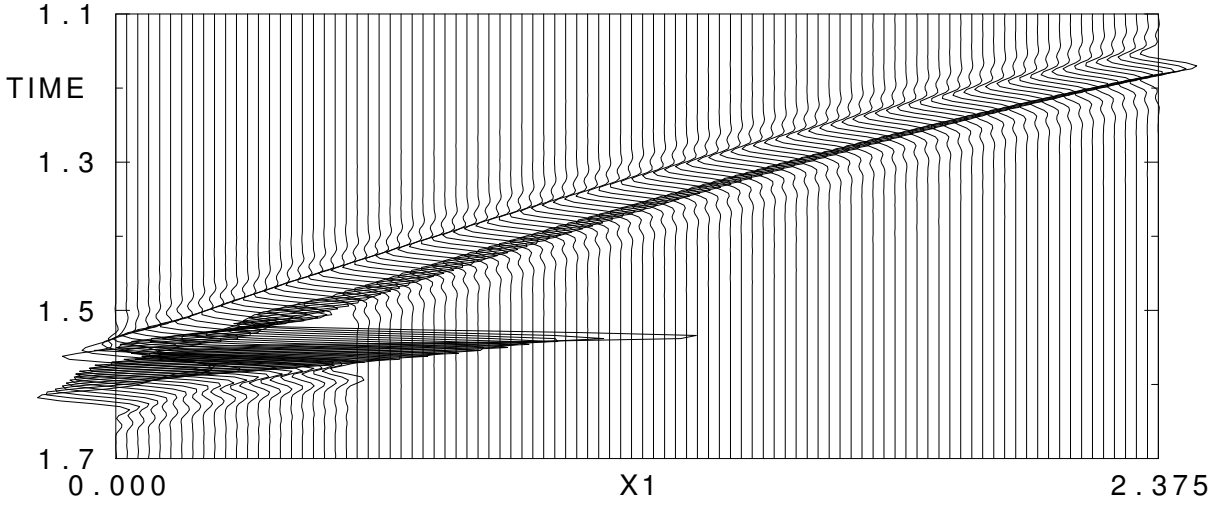

c)

Figure 4. Vertical component of synthetic seismograms of reflected P-wave for the single common-shot gather at line $x_2 = 5$ km corresponding to shot 80 ($x_1 = 4.975$ km) calculated in the model with **a)** triclinic anisotropy without the rotation and the P-wave velocity in the bottom layer 3.6 km/s, **b)** triclinic anisotropy with 15 degree rotation of the tensor of elastic moduli around the x_2 axis and the P-wave velocity in the bottom layer 3.6 km/s, and **c)** triclinic anisotropy with 15 degree rotation of the tensor of elastic moduli around the x_2 axis and the P-wave velocity in the bottom layer increased from 3.6 to 3.8 km/s. All seismograms have the same scaling.

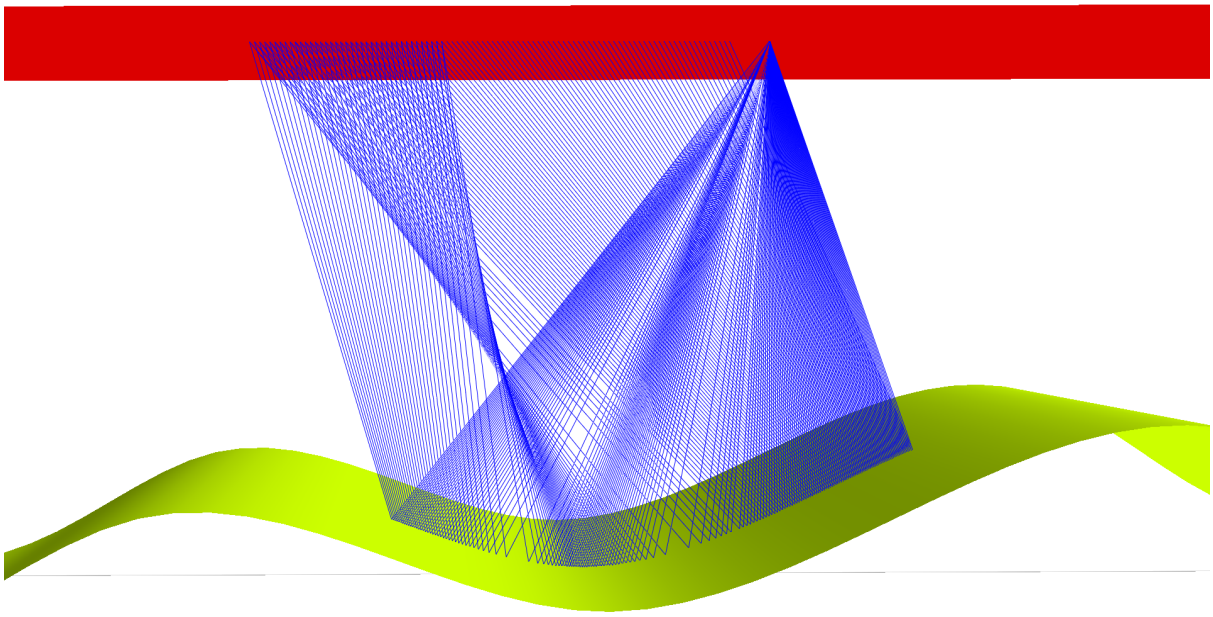

a)

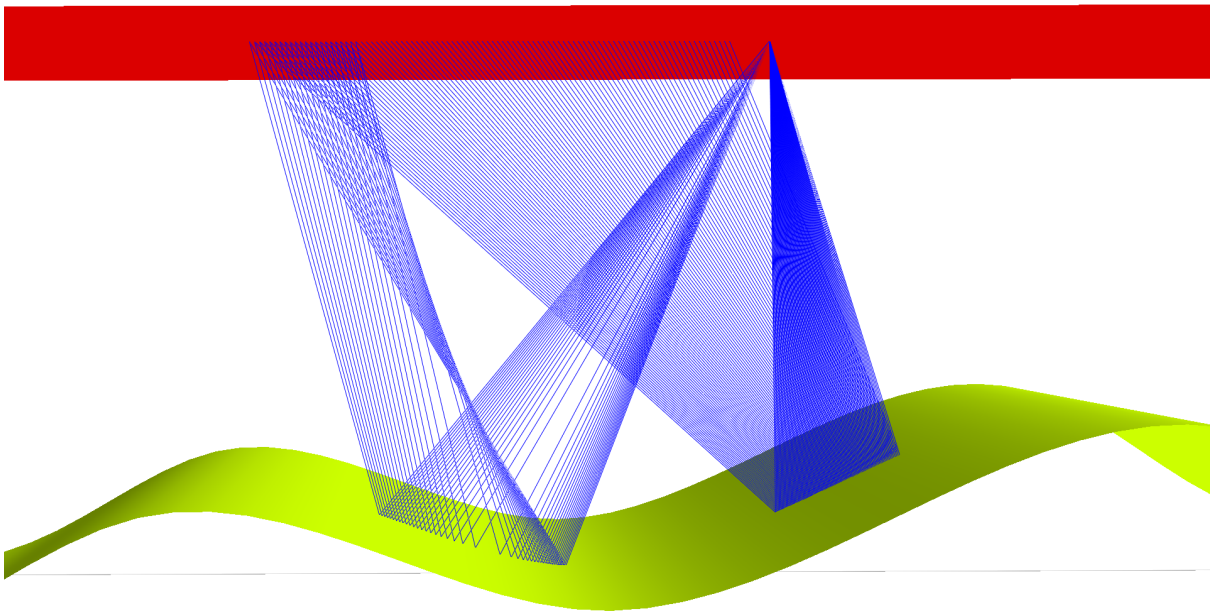

b)

Figure 5. Two-point rays of P-wave reflected from the curved interface calculated for the single common-shot gather at line $x_2 = 5$ km corresponding to shot 80 ($x_1 = 4.975$ km) in the model with **a)** triclinic anisotropy without the rotation and the P-wave velocity in the bottom layer 3.6 km/s, **b)** triclinic anisotropy with 15 degree rotation of the tensor of elastic moduli around the x_2 axis and the P-wave velocity in the bottom layer 3.6 or 3.8 km/s.

6. Conclusions

We have observed unexpected nearly vanishing part of the migrated interface in correct velocity model. The anisotropy of the model is triclinic with the rotation of the tensor of elastic moduli around the axis x_2. To explain the phenomenon, we have compared migrated images, synthetic seismograms and ray diagrams calculated for the selected common-shot gather. We have found out two causes of poorly displayed part of the migrated interface. The first cause is zero reflection coefficient and phase change which are responsible for the decrease of synthetic seismogram amplitudes. The second cause is the worse illumination of the interface by rays in the model with the 15 degree rotation of the tensor of elastic moduli.

We have already observed similar, nearly vanishing part of the migrated interface in *incorrect* velocity models (Bucha, 2012a, 2012b, 2013a) caused by different phenomenon. The poorly displayed part of migrated interface was caused by erroneous rotation of single common-shot images. When stacking the common-shot images, this rotation resulted in erasing the mentioned part of the interface due to the destructive interference.

Acknowledgments

The author thanks Luděk Klimeš and Ivan Pšenčík for help throughout the work on this paper.

The research has been supported by the Grant Agency of the Czech Republic under Contract P210/10/0736, by the Ministry of Education of the Czech Republic within Research Projects MSM0021620860 and CzechGeo/EPOS, and by the members of the consortium "Seismic Waves in Complex 3-D Structures" (see "http://sw3d.cz").

References

Bucha, V. (2011): Kirchhoff prestack depth migration in 3-D models: Comparison of triclinic anisotropy with simpler anisotropies. In: *Seismic Waves in Complex 3-D Structures, Report 21*, pp. 47–62, Dep. Geophys., Charles Univ., Prague, online at "http://sw3d.cz".

Bucha, V. (2012a): Kirchhoff prestack depth migration in 3-D simple models: comparison of triclinic anisotropy with simpler anisotropies. *Stud. geophys. geod.*, **56**, 533–552.

Bucha, V. (2012b): Kirchhoff prestack depth migration in velocity models with and without gradients: Comparison of triclinic anisotropy with simpler anisotropies In: *Seismic Waves in Complex 3-D Structures, Report 22*, pp. 29–40, Dep. Geophys., Charles Univ., Prague, online at "http://sw3d.cz".

Bucha, V. (2013a): Kirchhoff prestack depth migration in velocity models with and without vertical gradients: Comparison of triclinic anisotropy with simpler anisotropies In: *Seismic Waves in Complex 3-D Structures, Report 23*, pp. 45–59, Dep. Geophys., Charles Univ., Prague, online at "http://sw3d.cz".

Mensch, T. & Rasolofosaon, P. (1997): Elastic-wave velocities in anisotropic media of arbitrary symmetry-generalization of Thomsen's parameters ϵ, δ and γ. *Geophys. J. Int.*, **128**, 43–64.